THE DESCRIBING FUNCTION METHOD ACCURACY IN FIRST ORDER PLANTS WITH RATE-LIMITED FEEDBACK

M. Román, E. Ponce

Dept. Matemática Aplicada II, Universidad de Sevilla, Escuela Superior de Ingenieros
Camino de los Descubrimientos, 41092, Sevilla, Spain; Fax: (34) 954 48 61 65
E-mail: mroman@esi.us.es, enrique@ma2.us.es

Keywords: Nonlinear systems, rate-limiter, limit cycles, describing functions, bifurcations.

Abstract

In this paper, the rate limiter describing function is used to analyze by harmonic balance the existence of limit cycles in first order plants. Next, by comparison with analytical results previously obtained by the authors, the accuracy of the above approximate predictions is assessed. The main conclusion is that from a qualitative point of view the harmonic balance is good enough, providing in a exact way the critical value of the bifurcation parameter, and leading to neither spurious predictions of limit cycles nor failures in their detection. Regarding the quantitative aspects, the accuracy of the method depends on certain dimensionless parameter which is intrinsic to the problem.

1 Introduction

Rate-limiters are usual nonlinearities in control engineering due to the maximal speed of response of the actuators. Its presence in a dynamical system makes difficult its control, specially if the system is unstable, with special relevance in the study of the PIO problem (pilot-in-the-loop oscillations or pilot-induced oscillations), see for example [2].

As non-static nonlinearities, rate-limiters can be responsible for the appearance of limit cycles even for the case of first order plants. In this simplest case it is possible to show rigorously the existence of limit cycles as done in [7], but the application of the describing function method is not trivial. In this work, we make such frequency domain analysis for first order plants with rate-limited feedback and give some measures about the accuracy of its predictions, by comparing to the analytical results obtained in [7].

We study the system shown in Figure 1, where $y(t)$ is both the output of the linear system and the input of the nonlinear rate limiter, $z(t)$ is the output of the nonlinear block, $r(t)$ is a reference signal and $e(t)$ is the tracking error that becomes the input signal for the linear system. In the sequel it is assumed $r(t) = 0$ for all t, and therefore $e(t) = -z(t)$. Also note that both the gain factor k and the constant p will be assumed positive, to consider the important case where the system is open-loop unstable.

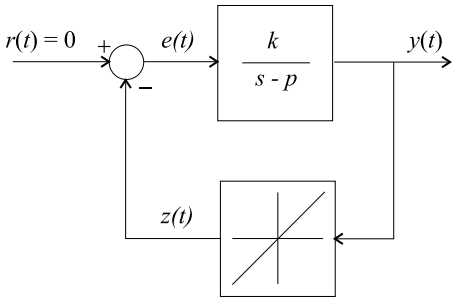

Figure 1: Block diagram of a first order linear system with a rate-limiter in the feedback loop.

The block in the feedback-loop of Figure 1 represents a rate-limiter whose output $z(t)$ tries to follow the input $y(t)$ but with restrictions in the maximal slope m that the output may have, so that, the slope of the output is to be bounded and satisfying $|\dot{z}| \leq m$. Thus, when the absolute value of the slope of the input overcomes the bound m, the output will separate from the input. Hence, the rate-limiter presents two operating modes clearly differentiated, according to whether the output is able to follow the input or not. In the first case we will say that the rate-limiter is in follower mode and we will refer to the second case as the nonfollower mode.

The structure of this work is as follows. In Section 2 we make the frequency domain analysis of the system. Next in Section 3 we present some analytical results to be used for the comparisons of Section 4. Some conclusions are offered at the end of the paper.

2 Frequency domain analysis

The frequency domain approach can be used to determine the conditions of existence of limit cycles in the system of Figure 1. To do this, we model the nonlinearity using its describing function ([8]) that can be obtained by computing the first harmonic of the output when the input is a sinusoidal waveform, see [4]. So, we need to know in a precise way the response of the rate-limiter to a periodic input. If the input y is greater that the output z, the output will grow at the maximum speed, ($\dot{z} = m$), and if $y < z$ then $\dot{z} = -m$. For a symmetrical sinusoidal input $y(t)$ with amplitude a and frequency ω, its time

derivative

$$\dot{y}(t) = a\omega \cos(\omega t) \tag{1}$$

does not violate the rate limiter bounds if $a\omega \leq m$, and therefore, then the output of the rate limiter follows its input. When $a\omega > m$ the bounds are violated and the output of the nonlinearity $z(t)$ is no longer able to follow exactly the input $y(t)$ during some periods, in which the output evolves at the maximum speed ($\dot{z} = \pm m$). Depending on the values of a, ω and m, three qualitatively different behavior modes of the output may exist, to be denoted as modes (a), (b) and (c), see [4].

We call mode (a) the case when the slope of the input $y(t)$ never violates the constrains $\pm m$, and so the input $y(t)$ and the output $z(t)$ coincide. This behavior mode is characterized by the condition $a\omega/m \leq 1$.

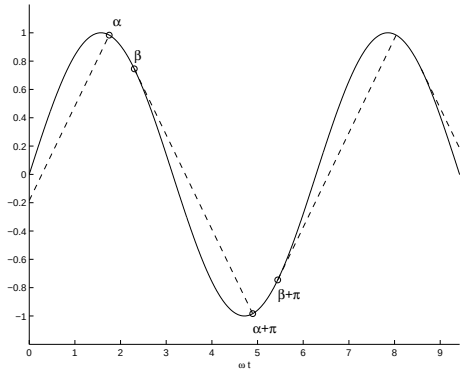

Figure 2: The output of the rate-limiter (discontinuous line) for a sinusoidal input (continuous line) in mode (b).

In mode (b) the output has time intervals in which it follows the sinusoidal input and intervals where it evolves as a straight line of slope $\pm m$. Assuming that the steady state has been reached, we denote by α and β the angles verifying $0 < \alpha < \beta < \pi$, associated to the extremes of the interval in which the rate-limiter is in follower mode, see Figure 2. The angle β corresponds to the separation of the output when the input is decreasing with $\dot{y} = -m$, and the angle α is such that $\alpha + \pi$ corresponds to the next intersection of the output with the input, assuming that the output has evolved at constant rate $-m$. Therefore, for the input $y(t) = a\sin(\omega t)$ the output is

$$z(t) = -a\sin(\beta) + m\left(t - \frac{\beta - \pi}{\omega}\right), \tag{2}$$

if $\beta - \pi < \omega t < \alpha$,

$$z(t) = y(t), \tag{3}$$

if $\alpha \leq \omega t \leq \beta$ or $\alpha + \pi \leq \omega t \leq \beta + \pi$,

$$z(t) = a\sin\beta - m\left(t - \frac{\beta}{\omega}\right), \tag{4}$$

if $\beta < \omega t < \alpha + \pi$, and so on periodically. From (1), since the slope of the input is $-m$ in $\omega t = \beta$, we have

$$\beta = \arccos\left(-\frac{m}{a\omega}\right) > \frac{\pi}{2}. \tag{5}$$

To determine the angle α, note that in $\omega t = \alpha + \pi$ occurs the intersection of the line with slope $-m$ with the sinusoidal input $y(t)$. We obtain after some manipulations the equation

$$\operatorname{sen}\alpha + \operatorname{sen}\beta = \frac{m}{a\omega}(\alpha + \pi - \beta). \tag{6}$$

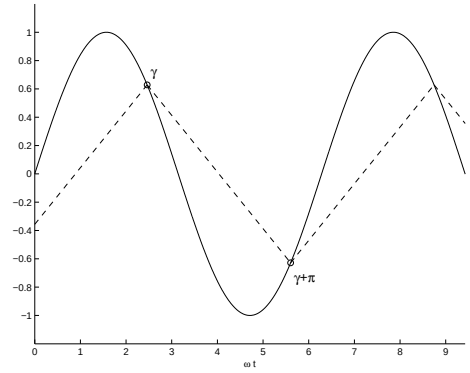

Figure 3: The output of the rate-limiter (discontinuous line) for a sinusoidal input (continuous line) in mode (c).

In mode (c) the input changes too fast and cannot be followed in any time interval of the steady regime response. Therefore, the output $z(t)$ evolves at the maximum rate $(\pm m)$ in both senses. Every time the output reaches the input, the slope of the output changes. Now, we denote the angle associated with the switching time by $\gamma \in (\pi/2, \pi)$, see Figure 3, and therefore, the output verifies

$$z(t) = -a\sin\gamma + m\left(t - \frac{\gamma - \pi}{\omega}\right),$$

if $\gamma - \pi < \omega t \leq \gamma$,

$$z(t) = a\sin\gamma - m\left(t - \frac{\gamma}{\omega}\right),$$

if $\gamma \leq \omega t < \gamma + \pi$,and so on periodically. To compute γ we use the continuity of the output in $\omega t = \gamma$ to obtain

$$\gamma = \arcsin\frac{\pi}{2}\frac{m}{a\omega}. \tag{7}$$

By moving parameters (a, ω, m), the transition between modes (b) and (c) occurs for a critical value $\gamma = \gamma^*$ when $\alpha = \beta = \gamma^*$. Applying (5), (6) and (7) and solving for the transition value of the dimensionless amplitude-frequency product, we obtain $(a\omega/m)^* = \sqrt{\pi^2/4 + 1} \approx 1.86$, and for the critical angle

$$\gamma^* = \arccos\left(\frac{-2}{\sqrt{\pi^2 + 4}}\right) \approx 2.14\,\text{rad}.$$

From the above analysis, it can be shown that depending on the value of the dimensionless parameter $a\omega/m$, only one mode is possible for the steady regime, more precisely:

Mode (a) if $0 < a\omega/m \leq 1$,

Mode (b) if $1 < a\omega/m < \sqrt{\pi^2/4+1}$, and

Mode (c) if $\sqrt{\pi^2/4+1} \leq a\omega/m < \infty$.

Notice that both in modes (b) and (c) there is a phase delay between the input and the output. This delay has an important effect in the global behavior mode of the nonlinearity.

2.1 Describing function of rate-limiters

Now taking the first harmonic of the output, the describing function can be obtained by computing

$$N(a,\omega) = \frac{1}{\pi a}\int_{-\pi}^{\pi} z(t)\, e^{j\omega t} d(\omega t),$$

where it must be taken into account the different possible modes of the rate-limiter. For the mode (b), and using (2), (3) and (4), we obtain

$$\begin{aligned}\mathrm{Re}\left[N(a,\omega)\right] = 2m\frac{\operatorname{sen}\alpha + \operatorname{sen}\beta}{\pi a\omega} + \\ + \frac{\operatorname{sen}\beta\cos\beta - \operatorname{sen}\alpha\cos\alpha + \beta - \alpha}{\pi},\end{aligned} \tag{8}$$

$$\mathrm{Im}\left[N(a,\omega)\right] = 2m\frac{\cos\alpha + \cos\beta}{\pi a\omega} + \frac{\operatorname{sen}^2\alpha - \operatorname{sen}^2\beta}{\pi}, \tag{9}$$

where α and β are defined in (5) and (6).

From (8) and (9) the describing function of the remaining modes can be easily deduced. In fact, taking $\alpha = 0$ and $\beta = \pi$, for mode (a) we obtain $N(a,\omega) = 1$.

For mode (c) it suffices to put $\alpha = \beta = \gamma$ in (8) and (9) to conclude that

$$N(a,\omega) = \frac{4m}{\pi a\omega}\left(\operatorname{sen}\gamma + j\cos\gamma\right),$$

where γ is defined in (7). Notice that in all modes the describing function depends only on the parameter $a\omega/m$, so that in the following we write $N(a,\omega) = N(a\omega/m)$.

2.2 Application to first order plants

The describing function method conjectures the appearance of a limit cycle of amplitude a and frequency ω for the solutions of the so-called harmonic balance equation. If $G(j\omega)$ is the frequency response function of the plant, for the system of Figure 1 we can write

$$G(j\omega) = \frac{-kp}{\omega^2+p^2} + j\frac{-k\omega}{\omega^2+p^2} = \frac{-1}{N(a\omega/m)}. \tag{10}$$

As is well known, the solution of this equation can be obtained graphically as the point in the Nyquist plot where the graph of $G(j\omega)$ intersects the locus of $-1/N(a\omega/m)$, as shown in Figure 4.

Due to the fact that $-1/N$ is always in the third quadrant, there will be a solution for (10) if and only if $G(0) = -k/p < -1$,

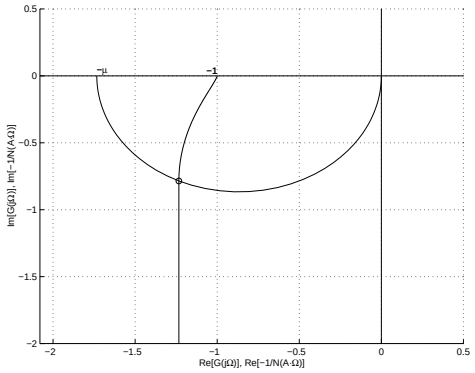

Figure 4: Graphic determination of the existence of limit cycles in the Nyquist Diagram.

with $k > p > 0$, that is, when the linear plant is open-loop unstable and closed-loop stable. Introducing now the dimensionless variables

$$A = \frac{ap}{m}, \qquad \Omega = \frac{\omega}{p},$$

together with the parameter $\mu = k/p$, we can write the harmonic balance equation (10) as

$$\frac{\mu}{\Omega^2+1} + j\frac{\mu\Omega}{\Omega^2+1} = \frac{1}{N(A\Omega)}, \tag{11}$$

leading to one limit cycle when $\mu > 1$, and to be solved for A and Ω as a function of μ. Now, we show the solutions of this system separately for each mode.

2.2.1 Mode (a)

As indicated before, the mode (a) occurs when the maximal slope of the sinusoidal input $a\sin(\omega t)$ is under the bound of the nonlinearity, that is, $a\omega \leq m$ or equivalently $A\Omega \leq 1$. In this mode the output of the rate-limiter is equal to the input and the describing function is obviously $N(A\Omega) = 1$.

System (11) becomes

$$\frac{\mu}{\Omega^2+1} = 1, \qquad \frac{\mu\Omega}{\Omega^2+1} = 0,$$

and the only possible solution is $\Omega = 0$ and $\mu = 1$, what suggests a degenerate situation for the limit cycle.

2.2.2 Mode (b)

In mode (b), we have $1 < A\Omega < (A\Omega)^* = \sqrt{\pi^2/4+1}$. Using the new variables A and Ω, we can rewrite (8) and (9), together with the conditions (5) and (6) but is not possible to obtain explicit expressions for the amplitude and the frequency as function of μ. Solving numerically for each value of $A\Omega$ in the considered range the transcendental equations defining α and β, one can compute the value of the describing function using

expressions (8) and (9). Then, from (11), we have

$$\Omega = \frac{\mathrm{Im}\left[1/N\left(A\Omega\right)\right]}{\mathrm{Re}\left[1/N\left(A\Omega\right)\right]}, \qquad \mu = \left(1+\Omega^2\right)\mathrm{Re}\left[1/N\left(A\Omega\right)\right].$$

Finally, the amplitude A can be computed from the value of the product $A\Omega$, that was the departure data. Following this process, by varying $A\Omega$ we can obtain the amplitude and the frequency as functions of μ.

2.2.3 Transition between modes (b) and (c)

For the critical value $(A\Omega)^* = \sqrt{\pi^2/4+1}$, the corresponding value of the describing function will be

$$N^* = \frac{4}{\sqrt{\pi^2+4}}\left(2 - j\frac{4}{\pi}\right).$$

Applying now (11) we obtain

$$\frac{\mu}{\Omega^2+1} = \mathrm{Re}\left(\frac{1}{N^*}\right) = \frac{\pi^2}{8},$$
$$\frac{\mu\Omega}{\Omega^2+1} = \mathrm{Im}\left(\frac{1}{N^*}\right) = \frac{\pi}{4}.$$

and solving for A, Ω, and μ we obtain the following values for the transition point

$$A^* = \frac{\pi}{4}\sqrt{\pi^2+4} \approx 2.92,$$
$$\Omega^* = \frac{2}{\pi} \approx 0.637,$$
$$\mu^* = \frac{\pi^2+4}{8} \approx 1.73.$$

2.2.4 Mode (c)

Using the new variables A and Ω, the describing function in mode (c) is

$$N\left(A\Omega\right) = \frac{4}{\pi}\frac{\mathrm{sen}\,\gamma + j\cos\gamma}{A\Omega}, \tag{12}$$

for $A\Omega > \sqrt{\pi^2/4+1}$, where γ verifies $\pi/2 < \gamma < \pi$ and

$$\gamma = \arcsin\frac{\pi}{2}\frac{1}{A\Omega}. \tag{13}$$

Now is possible to obtain explicit expressions for the amplitude and the frequency as functions of μ. Using (12) and (13) in (11), and solving for the amplitude and the frequency, we obtain

$$A = \frac{\pi}{2}\sqrt{\frac{8\mu}{8\mu-\pi^2}}, \qquad \Omega = \sqrt{\frac{8\mu}{\pi^2}-1},$$

for values of $\mu > \mu^* > \pi^2/8$, where μ^* is the above computed value for the bifurcation parameter corresponding to the transition between modes (b) and (c). Note also that when $\mu \to +\infty$ we have

$$A \to \frac{\pi}{2}, \qquad \Omega \to \infty.$$

3 Time domain analytical results

The dynamics of the linear plant in Figure 1 will be given by the differential equation

$$\dot{y} = py + ke = py + k\left(r - z\right) = py - kz, \tag{14}$$

where as usual the point denotes the derivatives with respect to the time, and we have had into account the negative feedback and the zero value of the reference signal $r\left(t\right)$.

In follower mode, the output follows the input while its slope does not overcome the bound, that is, $z\left(t\right) = y\left(t\right)$ if $\left|\dot{y}\left(t\right)\right| < m$. This situation will keep unchanged until that in some instant t_M the slope reach as the bound, that is, $\left|\dot{y}\left(t_M\right)\right| = m$. From this moment, if $\left|\dot{y}\left(t\right)\right| > m$, the output separates from the input and the nonlinearity enters the nonfollower mode, where the output evolves with constant slope, in the way

$$z(t) = z\left(t_M\right) + \dot{y}\left(t_M\right)\left(t - t_M\right),$$

that is with the maximal possible slope. The operation in nonfollower mode will continue up to some instant t_G, where the values of the input and the output coincide, that is, when $z(t_G) = y(t_G)$. If in this instant the slope of the input verifies $\left|y\left(t_G\right)\right| < m$, the output returns to reproduce the input (transition to the follower mode). But if $\left|y\left(t_G\right)\right| \geq m$, we will stay in nonfollower mode (with a possible transition of positive to negative nonfollower mode or vice-versa).

The above behavior leads to the nonlinear differential equation, which is valid for follower and nonfollower (positive or negative) modes and all the possible initial conditions

$$\dot{z} = \begin{cases} m\,\mathrm{sat}\left(\dfrac{\dot{y}}{m}\right) & \text{if} \quad y = z, \\ m\,\mathrm{sign}\left(y - z\right) & \text{if} \quad y \neq z. \end{cases} \tag{15}$$

Here 'sat' is the standard normalized saturation.

To describe the rate limiter nonlinearity some other authors (see [1]) simply take

$$\dot{z} = m\,\mathrm{sign}\left(y - z\right),$$

without any consideration about the meaning of this expression on the discontinuity line $y = z$. However, if one take into account the Filippov approach for sliding mode solutions, see [3], the above expression also leads to a description equivalent to equation (15).

Combining Equations (14) and (15) we have that the closed-loop dynamics will be given by the planar discontinuous dynamical system

$$\dot{y} = py - kz,$$
$$\dot{z} = \begin{cases} m\,\mathrm{sat}\left(\dfrac{py - kz}{m}\right) & \text{if} \quad y = z, \\ m\,\mathrm{sign}\left(y - z\right) & \text{if} \quad y \neq z, \end{cases} \tag{16}$$

which is symmetrical with respect to the straight-line $y = z$. The following result has been shown in [7]:

Theorem 1 *Consider system (16) with $k > 0$ and $p > 0$. The following statements hold.*

(a) If $0 < k < p$, then the origin is the only equilibrium point of the system and is unstable. There are no limit cycles and all the trajectories that do not point to the origin are unbounded.

(b) If $0 < k = p$, then all the points of the straight-line $y = z$ are (neutral) stable equilibrium points. Furthermore, all the solutions starting in the region $|y - z| < m/p$ are bounded and tend to one of the above equilibrium points as time goes to infinity; otherwise, solutions with initial conditions on the two connected components of the region $|y - z| \geq m/p$ are unbounded.

(c) If $0 < p < k$, then the origin is the only equilibrium point and is (not globally) asymptotically stable. There exists one unstable limit cycle surrounding the origin and limiting its attraction basin. The limit cycle is formed by two symmetric arcs that connect in a nonsmooth way at the points $(\pm m\theta/p, \pm m\theta/p)$, where θ is the unique positive solution of the transcendental equation

$$\theta \coth \theta = \frac{k}{k-p}.$$

Furthermore, the frequency of the limit cycle is

$$\omega = \frac{\pi p}{2\theta},$$

and its amplitude, measured as the maximal absolute value of the output of the system, is

$$a = \max(|y|) = \frac{mk}{p^2} \ln(\cosh \theta).$$

As a consequence of Theorem 1, we remark that for open-loop unstable systems, the existence of the rate-limiter precludes the possibility of the operating point to be globally asymptotically stable (G.A.S.). This fact is not very surprising since it also appears for other nonlinearities, see [5] and [6]. We conjecture that the same will be true for higher dimension in the plant.

Figure 5 shows the dimensionless values for the outputs of the plant and the nonlinearity, respectively, $\bar{y} = (p/m)\, y$ (continuous line) and $\bar{z} = (p/m)\, z$ (discontinuous line), versus the dimensionless time $\tau = pt$.

To facilitate the comparison of these results in the time domain (Theorem 1) with the results in the frequency domain, we compute the dimensionless amplitude and frequency as

$$A = \max(|\bar{y}|) = \frac{ap}{m} = \mu \ln(\cosh \theta), \qquad \Omega = \frac{\omega}{p} = \frac{\pi}{2\theta},$$

with

$$\theta \coth \theta = \frac{\mu}{\mu - 1}, \tag{17}$$

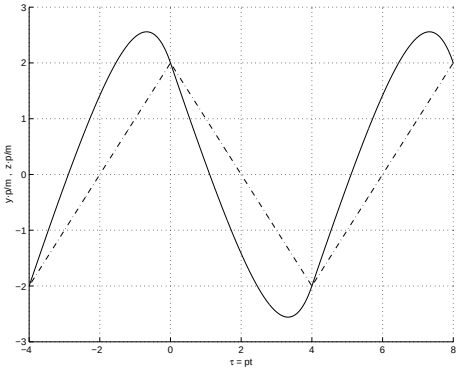

Figure 5: Time evolution of the limit cycle. It is shown the output of the plant (continuous line) and the output of the rate-limiter (discontinuous line).

for $\mu > 1$. Solving for μ in equation (17), substituting in the expression for the amplitude and taking the opportune limits for $\mu \to 1^+$ we have

$$\theta \to \infty, \qquad A \to \infty, \qquad \Omega \to 0,$$

and for $\mu \to +\infty$ we obtain

$$\theta \to 0, \qquad A \to \frac{3}{2}, \qquad \Omega \to \infty.$$

4 Comparison of the results

To check the accuracy of the obtained results using the describing function method we compare in Figures 6 and 7 the amplitude A and the frequency Ω, computed by the describing function method (discontinuous line) with those obtained by direct integration of the differential equations (continuous line). A circle onto the discontinuous line mark the supposed transition point between modes (b) and (c), as anticipated by the describing function method.

Figure 6 shows for the amplitude a reasonable level of accuracy between both methods. Note that the birth of the limit cycle occurs with infinite amplitude. A detailed analysis shows that the amplitude computed by the two methods there are not of the same order, due the limit cycle is no very sinusoidal when it is born. That is a limitation of the describing function method.

In Figure 7 we see for the frequency a good level of accuracy between both methods. Note that the birth of the limit cycles occurs with null frequency (the limit cycle is not very sinusoidal at the bifurcation point).

Remembering that the exact value for the amplitude for μ sufficiently great is $3/2$ and the one computed using harmonic balance is $\pi/2$, the limit of the relative error for the amplitude far away the bifurcation point is $(\pi - 3)/3 \approx 0.047 < 5\%$.

We find the following qualitative difference: for small values of the bifurcation parameter the describing function method conjectures the existence of limit cycles in mode (b) (combining both follower and nonfollower modes), and limit cycles

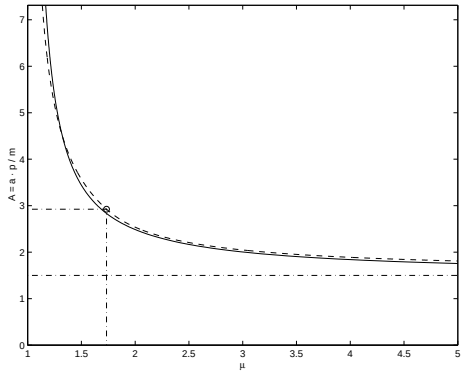

Figure 6: Adimensional amplitude computed with the describing function method (discontinuous line) and by integrating the system (continuous line).

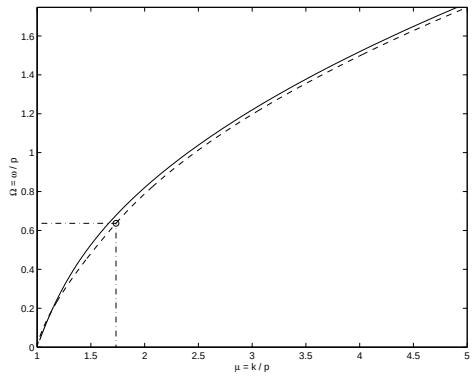

Figure 7: Dimensionless frequency computed with the describing function method (discontinuous line) and by integrating the system (continuous line).

in mode (c) (using only nonfollower mode) for big values of the bifurcation parameter. However, integrating the differential equations of the system we have found that the limit cycle is always of the same nature (using only nonfollower mode) for all the values of the bifurcation parameter greater than the critical one. This inaccuracy is due to the fact that the describing function method provides a good approximation to the first harmonic of the true output signal and so it have a serious handicap when the true signal is very different from its first harmonic. In our case the birth of the limit cycles (small values of the bifurcation parameter) occurs with waveforms very far from sinusoidal.

5 Conclusions

We have considered a dynamical system composed by a linear first order plant and a rate-limiter in the feedback loop. From the nonlinear differential equation of the rate-limiter in the time domain we state previously obtained results about existence, amplitude and frequency of the limit cycle (Theorem 1). The proof of this result will appear elsewhere.

We have show how to apply the describing function method in order to characterize the existence, amplitude and frequency of the existing cycle.

Comparing both methods, our principal conclusion is that for large μ (that is, $\mu \geq \mu^*$) the describing function method provide explicit solutions with only a minor quantitative inaccuracy. For small μ (that is, $1 < \mu < \mu^*$), the implicit solution obtained using the describing function method is more difficult to use than the solution obtained by integrating the differential equations. Also, the quantitative and qualitative discrepancies between the describing function method and the exact analytical results increase when the bifurcation parameter μ tends to its critical value ($\mu = 1$).

Acknowledgments

The authors wish to thank professors E. Freire, J. Aracil and F. Gordillo for their comments and suggestions to a preliminary version of the manuscript. This work has been partially supported by the Spanish Ministry of Science and Technology under the grant DPI-2000-1218-C04-04.

References

[1] J. Ackermann, T. Bünte. "Robust prevention of limit cycles for robutsly decoupled car steering dynamics", *Proc. 5th IEEE Mediterranean Conference on Control and Systems, Paphos, Cyprus,* (1997).

[2] H. Duda, "Flight control system design considering rate saturation", *Aerospace Science and Technology,* **4**, pp. 265-275, (1998).

[3] A. F. Filippov, *Differential Equations with Discontinuous Righthand Sides,* Mathematics and its Applications. Kluver Academic Publishers, Dordretch, The Netherlands, (1988).

[4] F. Gordillo, I. Alcalá, J. Aracil, "Bifurcations in systems with a rate limiter", *in Dynamics, Bifurcations and Control,* F. Colonius and L. Grüne (Eds.), pp. 37-50, LNCIS 27, Springer, New York, (2002).

[5] D. Pagano, E. Ponce, J. Aracil, "Bifurcation analysis of time delay control systems with saturation", *International Journal of Bifurcation and Chaos,* **9**, pp. 1089-1110, (1999).

[6] E. Ponce, J. Aracil, D. Pagano, "Control systems with actuator saturation and bifurcation and infinity", *Proceedings of the Seventh Mediterranean Conference on Control and Automation, Haifa, Israel,* pp. 1598-1608, (1999).

[7] M. Román, E. Ponce, "Limit cycles in first order systems with rate-limiter in the feedback loop", *Preprint,* (2002).

[8] J.-J. Slotine, W. Li, *Applied Nonlinear Control,* Prentice Hall Inc., (1991).